Collection efficiency of scattered light in single-ended optical fiber sensors

Sasani Jayawardhana, Alexander P. Mazzolini, and Paul R. Stoddart*

Faculty of Engineering and Industrial Sciences, Swinburne University of Technology, Hawthorn, Victoria 3122, Australia
**Corresponding author: pstoddart@swin.edu.au*

Received May 20, 2011; revised February 22, 2012; accepted March 23, 2012;
posted March 23, 2012 (Doc. ID 147935); published June 1, 2012

Optical fibers allow a variety of spectroscopic sensing methods to be implemented in a single-ended backscattering geometry. Taking multimode fibers with surface-enhanced Raman scattering active tips as a model system, it is shown that the remote single-ended collection geometry can be relatively inefficient in comparison to the performance of the underlying sensor structure. Therefore the performance of the single-ended geometry has been compared to the analogous sensor structure on a nonguiding silica glass substrate. While part of the reduction in collection efficiency can be attributed to mismatches between the numerical aperture of the collection optics and that of the fiber, this study suggests that there can be an additional loss due to a mismatch between the confocal area of the collection optics and the area of the fiber core. This effect is most significant for high numerical aperture objectives. However, the collection efficiency is somewhat higher than would be expected from a simple area ratio analysis. This can be attributed to the graded-index fiber used in the model system and the relaxation of confocal requirements in the longitudinal direction.

OCIS codes: 060.2370, 300.6450, 130.6010, 180.5655.

Optical fibers provide an excellent platform to implement a number of spectroscopic methods for sensing applications [1]. The sensing point can be spatially separated from the user during measurement, allowing it to be used in a single-ended or "remote" sensing arrangement. This is particularly useful when dealing with hazardous materials [2] or in biomedical applications [3]. However, signal collection from an optical fiber sensor with an active tip may be complicated by the light guiding properties of the optical fiber and the losses associated with coupling scattered light through to the detector. The factors that determine signal collection through an optical fiber have not been thoroughly investigated, despite their importance for sensor optimization. The present work uses surface-enhanced Raman scattering (SERS) as a model sensing system to investigate the signal collection efficiency from multimode graded-index (GRIN) optical fibers. SERS provides a sensitive and selective method for detecting analytes at trace levels [4]. Earlier work on the fabrication of SERS substrates on fiber tips using oblique angle deposition (OAD) [5] has shown that the signal collected remotely through the fiber can be substantially lower than that obtained by direct measurements of the SERS substrate, as shown in Fig. 1.

Even with thin metal layers where reflection losses at the glass—metal interface were small, the remote geometry provided only about 7% of the signal level measured directly from the SERS substrate [5]. The earlier work employed a 50× long working distance objective with a numerical aperture (NA) of 0.5, which is representative of a typical lens for Raman spectroscopy. In the current study, the same objective is used to interrogate single-ended optical fiber SERS sensors in order to analyze the collection efficiency discrepancy in more detail.

The remote signal collection efficiency for a SERS fiber can be expressed as follows:

$$I'_{\text{fiber}} \propto G' \int_{\Omega_{\text{fib}}} \frac{d\sigma}{d\Omega} \mathrm{d}\Omega \int_0^{\infty} \int_0^{2\pi} \int_0^{\rho} f(r,\theta,z) r \mathrm{d}r \mathrm{d}\theta \mathrm{d}z,$$

where I'_{fiber} refers to the measured intensity of the scattered light collected through the optical fiber, normalized against the laser excitation power at the SERS substrate. In this case, it is understood that proper evaluation of the laser excitation power must take into account the loss due to coupling the laser excitation into the optical fiber. G' refers to the SERS enhancement factor in the remote measurement. Once the Raman-shifted light is scattered into the far-field, only the fraction of light that is confined within the numerical aperture of the optical fiber will be guided back towards the objective. This is accounted for by the integration of the differential scattering cross-section ($d\sigma/d\Omega$) over the collection cone of the fiber (solid angle Ω_{fib} in steradians). The volume integral of $f(r,\theta,z)$ is referred to here as the overlap fraction and defines the overlap between the collection cone of the objective and the spatial distribution of the scattered light.

Assuming that the scattering cross-section is constant (isotropic scattering), the above expression can be simplified to

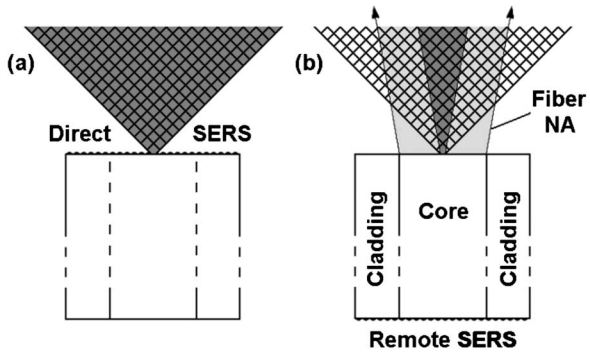

Fig. 1. Schematic diagram of (a) direct and (b) remote single-ended SERS measurement geometries. The hatched region represents the collection cone of the microscope objective, while the dark-shaded region shows the portion of the SERS signal that is captured by the objectives in each case.

$$I'_{\text{fiber}} \propto G' \frac{d\sigma}{d\Omega} \Omega_{\text{fib}} \int_0^{\infty} \int_0^{2\pi} \int_0^{\rho} f(r,\theta,z) r \mathrm{d}r \mathrm{d}\theta \mathrm{d}z. \quad (1)$$

In contrast, the signal collection efficiency for a direct measurement from the SERS-active surface would be

$$I \propto G \int_{\Omega_{\text{obj}}} \frac{d\sigma}{d\Omega} \mathrm{d}\Omega = G \frac{d\sigma}{d\Omega} \Omega_{\text{obj}}, \quad (2)$$

where G refers to the SERS enhancement in the direct excitation and the overlap fraction is set to unity by definition.

Dividing Eq. (1) by Eq. (2) leaves a ratio

$$\left(\frac{I'}{I}\right)_{\text{fiber}} = \frac{G'}{G} \left(\frac{\Omega_{\text{fib}}}{\Omega_{\text{obj}}}\right) \int_0^{\infty} \int_0^{2\pi} \int_0^{\rho} f(r,\theta,z) r \mathrm{d}r \mathrm{d}\theta \mathrm{d}z. \quad (3)$$

The corresponding ratio for a SERS substrate on a nonwaveguiding substrate would be $(I'/I)_{\text{slab}} = G'/G$. This simplified expression allows the main contributions to the discrepancy between remote and direct measurements to be isolated and analyzed.

Note that in general the SERS process may be anisotropic (see, e.g., [6]). Although it may be of interest to include a more exact expression for the differential scattering cross-section in future work, the signal is expected to be approximately constant for scattering angles close to 180°. Therefore the assumption of isotropic scattering is only expected to make a second-order contribution to the overall discrepancy.

SERS substrates were fabricated using cleaved fiber sections of 25 ± 1 mm length (62.5/125 μm core/clad diameter, NA = 0.272). One tip of each section was coated with silver (99.95%, Goodfellow) using OAD [5]. A 10 mM ethanolic solution of thiophenol (99%+, Merck) was used as the test analyte, as thiophenol forms stable monolayers on silver surfaces. Fig. 2 shows typical thiophenol spectra obtained in the direct and remote interrogation geometries for a SERS fiber. A Renishaw InVia Streamline microscope with a wavelength of 514 nm was used for the acquisition of spectra, while a Horiba Jobin-Yvon (HJY) modular microscope (532 nm) was used to obtain the depth profiles to infer the size of the confocal region. The conventional pinhole arrangement of the HJY avoided any potential confusion that might arise when using the virtual pinhole of the Renishaw system to probe the waveguide structure. Nevertheless the two instruments were found to provide comparable confocal behavior, and the difference in the two excitation wavelengths has a negligible effect on the following analysis of the diffraction-limited spot size.

The direct and remote measurements from the optical fiber were compared to the analogous measurements from substrates fabricated on nonwaveguiding silica glass cover slips. Although the direct measurement of the signal intensities on the optical fiber and the cover slip (Fig. 3) are somewhat different, this is to be expected due to the differences in OAD film growth. Nevertheless, as the emphasis here is on the relative efficiency between the direct and remote measurement geometries in each case, small differences in the SERS substrates are not expected to have a significant effect on the overall conclusion.

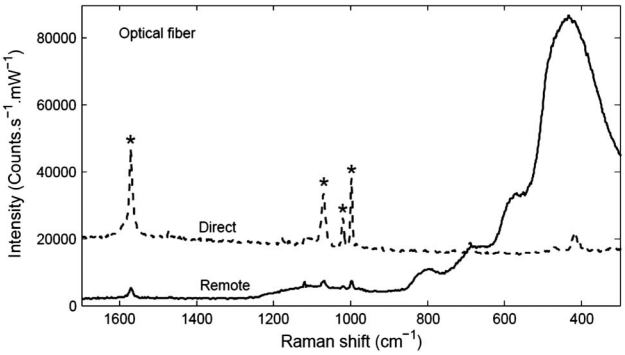

Fig. 2. Thiophenol SERS spectra taken from an OAD substrate with average island height of 31 ± 5 nm on an optical fiber tip. The four thiophenol peaks used to quantify the signal amplitude are shown by asterisks. The broad silica background from the optical fiber peaks at 430 cm^{-1} in the remote measurement. The spectra have been vertically offset for clarity.

For spectra acquired using the cover slip, the remote signal intensity was consistently higher than that of the direct signal by a factor of 3.0, which provides the ratio G'/G for use in Eq (3). Similar observations of higher SERS enhancements for reverse excitation have been reported previously [7].

In comparison, the ratio between remote intensity and direct intensity measurements from the optical fiber normalized to the coupled laser power is $(I'/I)_{\text{fiber}} = 0.14$ (Fig. 2). The overlap fraction in Eq. (3) can now be isolated by dividing this ratio by the collection aperture factor $\Omega_{\text{fib}}/\Omega_{\text{obj}}$ and the SERS enhancement factor obtained from the cover slips. The resulting value of 0.17 is significantly lower than unity, which implies that the objective used in this study does not efficiently capture the light emitted by the optical fiber.

The scattered signal that is guided back through the optical fiber may emerge at any point across the fiber core. However, at the proximal end face only the rays that fall within the projected area of the confocal pinhole will be passed through to the detector. In a simplified model of a uniform illumination of the sensor surface and a one-to-one mapping of the scattered signal on to the proximal end of the fiber, the collection efficiency can be thought of as an area fraction. This amounts to a geometrical mismatch between the confocal sampling area ($A_{\text{conf}} = \pi\rho^2$,

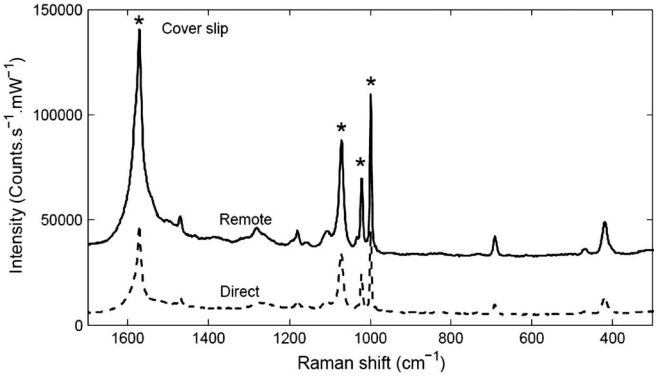

Fig. 3. Thiophenol SERS spectra taken from similar OAD substrates on a cover slip. Spectra are vertically offset for clarity.

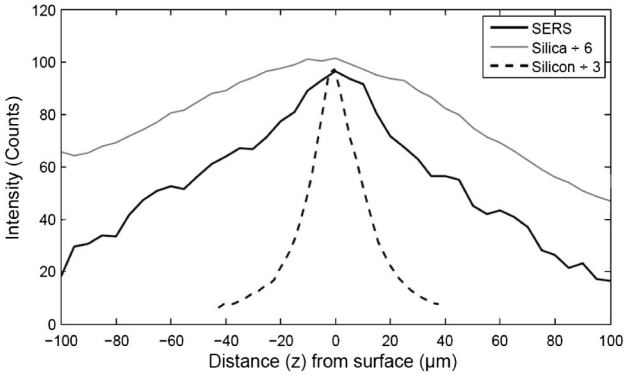

Fig. 4. Comparison of a silicon depth profile with profiles through the remote end of the optical fiber. Negative depth indicates focusing below the surface. The SERS peak intensity of thiophenol at 1000 cm^{-1} and the silica Raman background intensity at 430 cm^{-1} are plotted together with the height of the 520 cm^{-1} peak of silicon. Measurements were acquired using an integration time of five seconds and three averages.

where ρ is the radius of the confocal spot) and the fiber core area ($A_{core} = \pi a^2$ where a is the fiber core radius).

Note that the diameter of the confocal spot is different to that of the diffraction-limited focal point of the laser. For the 50× objective (0.5 NA), the diffraction-limited spot is 1.3 μm [8]. However, according to Juang *et al.*, the limiting depth resolution is related to the full-width half-maximum of a standard confocality measurement [9]. In the present study, there is a significant difference between the diffraction-limited depth resolution (2.1 μm), and the experimentally measured value of 21.5 μm from the depth profile shown in Fig. 4. Part of the reason for this difference is the relatively large 400 μm pinhole that is used to avoid excessive loss of signal. Therefore, given that the actual confocal depth is 10 times larger than the diffraction-limited resolution (21.5 μm:2.1 μm), the same factor is expected to apply to the confocal spot size relative to the diffraction-limited spot. This gives an effective confocal spot size of 13 μm, which would result in a collection efficiency of 4.3% from the proximal end face, based on the area fraction $(\rho/a)^2$.

Clearly, an area fraction of 0.043 is significantly lower than the measured overlap fraction of 0.17. Two additional factors that may account for this discrepancy are the relaxation of confocality in the longitudinal direction and the waveguiding nature of the graded-index optical fiber. These factors can be used to refine the collection efficiency distribution function $f(r, \theta, z)$ in Eq. (3).

It is known that transparent samples behave differently from opaque samples when interrogated through a confocal microscope [10], due to the contribution from the signal generated within the extended illumination cone. This contribution is evident from Fig. 4, where the depth profiles of the SERS signal and the silica Raman background appear broadened with respect to the standard silicon profile. Bridges *et al.* used a geometrical relationship to quantify the multiplicative contribution of the out-of-focus signals originating from a silica slab [11]. This term represents the z-dependence of the collection efficiency distribution function $f(r, \theta, z)$:

$$E(z) = [1 + (z/l)^2]^{-1}, \tag{4}$$

where $E(z)$ is the overall signal detection efficiency from the plane at distance z from the focus, and l is defined as the depth of focus. To a first approximation, the same equation can be used for the cylindrical waveguide presented here, as the internal reflections of light rays inside the fiber core can be thought of as a folded version of the collection cone in the analysis of [11]. The infinite integral of Eq. (4) yields a value of 1.5, which can be argued to be an upper limit for this factor.

In addition, the refractive index profile of the GRIN fibers used in this work tends to focus the guided light towards the core center [4]. A simple geometrical analysis of line scans across a graded-index fiber shows that the signal collected from the center of the fiber core using a 50× objective can be weighted by a factor of $\xi = 2.58$ in comparison to a uniform illumination. The theoretical overlap fraction now becomes

$$\int_0^{\infty}\int_0^{2\pi}\int_0^{\rho} f(r,\theta,z) r \mathrm{d}r\mathrm{d}r\mathrm{d}\theta\mathrm{d}z = \xi\left(\frac{\rho}{a}\right)^2 \int_0^{\infty} E(z)\mathrm{d}z = 0.17,$$

which is in agreement with the measured value.

The results of this study may assist in the selection and optimization of optical fibers for use in single-ended optical fiber sensors. While it is common practice in normal Raman micro-spectroscopy to use high NA objectives to improve the collection efficiency of the scattered light, the present results suggest that this may be counterproductive in the case of optical fiber SERS probes. In particular, it appears that high NA fibers with small mode field diameters (e.g. single-mode fibers) might be preferable to the multi-mode fibers commonly used in the field [4]. Proper matching of the objective NA and magnification to the optical fiber specifications should also be considered. However, the advantages of this approach would have to be weighed against the associated levels of fiber Raman background and the increased coupling losses associated with single mode fibers.

This work was supported by the Australian Research Council (DP1092955) and National Health and Medical Research Council Development Grant 499321.

References

1. R. A. Potyrailo, S. E. Hobbs, and G. M. Hieftje, Fresenius J. Anal. Chem. **362**, 349 (1998).
2. D. A. Stuart, K. B. Biggs, and R. P. Van Duyne, Analyst **131**, 568 (2006).
3. D. L. Stokes and T. Vo-Dinh, Sens. Actuators B **69**, 28 (2000).
4. P. R. Stoddart and D. J. White, Anal. Bioanal. Chem. **394**, 1761 (2009).
5. S. Jayawardhana, G. Kostovski, A. P. Mazzolini, and P. R. Stoddart, Appl. Opt. **50**, 155 (2011).
6. Y. J. Liu, J. G. Fan, Y. P. Zhao, S. Shanmukh, and R. A. Dluhy, Appl. Phys. Lett. **89**, 173134 (2006).
7. C. Jennings, R. Aroca, A. M. Hor, and R. O. Loutfy, Anal. Chem. **56**, 2033 (1984).
8. N. Everall, Spectroscopy **19**, 22 (2004).
9. C. B. Juang, L. Finzi, and C. J. Bustamante, Rev. Sci. Instrum. **59**, 2399 (1988).
10. N. Everall Appl. Spectrosc. **62**, 591 (2008)
11. T. E. Bridges, M. P. Houlne, and J. M. Harris, Anal. Chem. **76**, 576 (2004).